Progress In Electromagnetics Research C, Vol. 112, 193–205, 2021

Compact Quad-Port High Performance UWB MIMO/Diversity Antenna with Slotted Ground Structure

Pankaj K. Keshri[1], Richa Chandel[2, *], Sanjay Sahu[1], and Anil K. Gautam[3]

Abstract—A compact $30 \times 30\,\text{mm}^2$ high performance four elements ultra-wide band multi-input multi-output (UWB MIMO) diversity antenna is proposed. The prototype antenna consists of four symmetrical antenna elements which are orthogonally placed on top surface of the substrate with partial slotted ground plane. The isolation among the antenna elements is improved by placing antenna elements orthogonally without any additional decoupling structure. The various antenna characteristic parameters, i.e., return loss ($< -10\,\text{dB}$), isolation parameter ($< -22\,\text{dB}$), radiation patterns near omnidirectional, and maximum realized gain 4.8 dB, were measured. The MIMO performances of prototype antenna were also measured in terms of various MIMO diversity parameters and found ECC < 0.06, DG $> 9.98\,\text{dB}$, TARC $< -10\,\text{dB}$ and MEG $< -3\,\text{dB}$ throughout the frequency band. This design provides an operational bandwidth from 2.15 to 16.75 GHz which covers the whole UWB spectrum and is suitable for portable devices.

1. INTRODUCTION

Ultra-Wide Band (UWB) technology is quite suitable for short range wireless communications like personal area network applications. The Federal Communications Commission (FCC) decided 3.1–10.6 GHz as unlicensed frequency range for UWB in 2002 [1]. High data rate, large bandwidth, and low power spectral density are the advantages of UWB which is suitable for today's wireless communication portable devices. In spite of various advantages of UWB technology, it also has certain limitations observed like multipath fading system and reliability. These problems are resolved by combining UWB technology with MIMO technology. In MIMO system, multiplexing and diversity gain increase as multiple antennas are used at both the sender side and receiver side which in turn increases transmission capacity. Since accommodating the multiple antenna to a small area leads to chances of coupling among the antenna elements, it is a big challenge for antenna designers to design a miniature MIMO antenna with low coupling between the antenna elements. In [2], Y-shaped slots are used in a half slot CPW feed MIMO antenna to improve isolation. In [3], isolation is improved by using a complementary split-ring resonator (CSRR) and an inverted L-stub on the ground plane. Two perpendicular meander feed lines on single radiator and open stub at the corner of structure are used to improve isolation parameter in [4]. An array of slotted Y-shaped frequency selective surfaces along with an inverted L-structure provides isolation among the antenna elements [5], in which antenna elements are designed around a polystyrene block in a cuboidal geometry. Some other techniques are also used for isolation improvement like neutralization line between antenna elements [6], electromagnetic bandgap structure [7, 8], introducing various defective ground structure (DGS) or stub and slot on antenna elements [9–14]. For isolation improvement, a carbon black film is used, and it absorbs electromagnetic signal [15]. In [16, 17], a metamaterial, which is an artificial structure and magneto dielectric material, is used to decrease the

Received 4 March 2021, Accepted 6 May 2021, Scheduled 12 May 2021
* Corresponding author: Richa Chandel (richachandel23@gmail.com).
[1] Lovely Professional University, Phagwara, Punjab, India. [2] University Institute of Technology, Himachal Pradesh University, Shimla, India. [3] G. B. Pant Institute of Engineering and Technology, Pauri Garhwal, Uttarakhand, India.

mutual coupling by absorbing mutual interference signal. A DGS and U-shaped stubs are inserted on radiator [18, 19] whereas a decoupling structure is used on top and bottom surfaces of the dielectric substrate to improve an isolation as well as bandwidth of the UWB MIMO antenna in [20]. Further, the overall size of the antenna is decrease by using asymmetric coplanar strip (ACS)-fed structure [21]. In [22–24], antenna elements are placed orthogonally to enhance the isolation. It is a big challenge to design a MIMO antenna in compact size with low mutual coupling. The performance of prototype antenna compared with existing literature in terms of antenna size, frequency band, isolation, and ECC is shown in Table 1. It can be seen that the size of proposed antenna is very compact compared to all other antennas. In addition, it also shows better performance in achieving high isolation, low ECC value, and high gain which is favorable for today wireless portable devices.

Table 1. Comparison of performance of prototype antenna with existing literature.

Existing literature	Antenna size (mm^2)	Frequency band (GHz)	No. of port	Isolation (dB)	Gain (dBi)	ECC
[5]	$32 \times 36 = 1152$	3–10	4	< -20	—	< 0.002
[6]	$48 \times 34 = 1632$	3.52–10.08	4	< -23	0.95–2.91	< 0.039
[7]	$27.2 \times 46 = 1251$	3.6–17.6	2	< -18	1.4–4	< 0.018
[8]	$60 \times 60 = 3600$	3–16.2	4	< -17.5	8.4	< 0.300
[15]	$50 \times 40 = 2000$	2.5–11	2	< -15	4.6	< 0.01
[18]	$80 \times 80 = 6400$	3.18–11.5	4	< -15	6	< 0.005
[19]	$80 \times 35 = 2800$	2.57–12.2	2	< -15	3.06–4.6	< 0.005
[20]	$40 \times 40 = 1600$	3.1–11	4	< -20	3.28	< 0.002
[21]	$36 \times 36 = 1296$	3.1–10.6	4	< -15	3.7	< 0.02
[22]	$26 \times 55 = 1430$	3.1–12.3	4	< -20	4.2	< 0.10
[23]	$50 \times 39.8 = 1990$	2.7–12	4	< -17	6	< 0.02
[24]	$39 \times 39 = 1521$	2.3–13.75	4	< -22	4.6	< 0.02
Proposed Antenna	$30 \times 30 = 900$	2.15–16.75	4	< -22	1.2–4.8	< 0.06

In this paper, a very compact $30 \times 30\,mm^2$ quad-port UWB MIMO/diversity antenna without using any additional decoupling structure which unnecessarily increases the complexity and size of antenna is proposed. The great amount of isolation is achieved by placing four identical antenna elements orthogonally and cutting arc-shape on the radiator, due to which interference is reduced via polarization diversity. The bandwidth of antenna is improved by modifying ground plane and cutting a slot in ground plane at an optimum position to alter the surface current distribution. The compactness is achieved due to a staircase shaped structure cut at bottom corners of the radiating patch. The prototype antenna has very high bandwidth ranging from 2.15 to 16.75 GHz, high isolation, and very low ECC value which is suitable for modern communication devices especially for portable UWB-MIMO devices.

2. ANTENNA DESIGN PROCEDURE

The structure of a $30 \times 30 \times 1.6\,mm^3$ four element MIMO antenna is presented in Figure 1. The design consists of four identical antenna elements which are orthogonally placed on top surface of the substrate, and ground structure is modified by cutting a slot at a suitable position. The design and simulation work are carried out on ANSYS HFSS full wave electromagnetic simulator, and optimized dimensions are presented in Table 2.

The proposed radiating element consists of a rectangular patch of length (L_p) and width (W_p) etched with an arc shaped radiator in order to improve the bandwidth. Further, truncated stair case

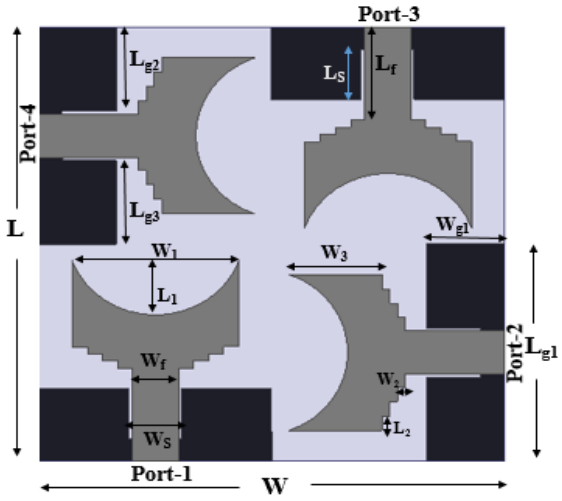

Figure 1. Structure of four element MIMO antenna with dimension.

Table 2. Optimized dimension of proposed antenna.

Parameter	L	L_f	L_{g1}	L_{g2}	L_{g3}	L_1	L_2	L_S
Dimensions (mm)	30	6.4	15	5.8	5.8	3.8	1	3.5
Parameter	W	W_f	W_{g1}	W_S	W_1	W_2	W_3	
Dimensions (mm)	30	3	5	3.4	10.8	0.5	6	

shaped slots are etched on the radiator to increase the path of current and hence reduce the size of antenna. In order to obtain lower cutoff frequency, the size of the antenna should be large enough to provide the longest current path. In this paper, a lower frequency rectangular shaped slot of length and width of ($L_S \times W_S$) is etched on the partial ground. A microstrip-line of length and width of L_f and W_f is connected at the lower middle edge of the radiator. The approximate lower resonant frequency for the proposed antenna is evaluated by [25],

$$f_r = \frac{14.4}{l_1 + l_2 + g + \dfrac{A_1}{2\pi l_1\sqrt{\varepsilon_{re}}} + \dfrac{A_1}{2\pi l_2\sqrt{\varepsilon_{re}}}} \tag{1}$$

where l_1 and l_2 denote the length of ground plane and length of patch; A_1 and A_2 denote the area of ground plane and radiating patch; g denotes the gap between radiating patch and ground plane; $\varepsilon_{re} = (\varepsilon r + 1)/2$ denotes the relative permittivity. The lower resonant frequency obtained from above formula is 5.8 GHz by inserting the value $l_1 = Lg_1$, $l_2 = Lp$, $g = L_f - Lg$, $A_1 = Lg_1Wg_2 - L_sW_s$, $A_2 = LpWp + L_fW_f - 2 * \{(L_2W_2) + (2 * L_2W_2) + (3 * L_2W_2)\} - 0.5 * \pi * r^2$, which is very close to simulated value 5.6 GHz as shown in Figure 4(a).

2.1. Evolution Steps of Single UWB Antenna

The various evolution steps of single UWB antenna are presented in Figure 2. In step-1, the antenna design starts with a basic rectangular patch whose dimension is 7.5 mm × 10.8 mm, and it resonates around 4.4 GHz. After removing an arc shaped slot in step-2 and including a staircase structure in step-3, the resonating frequency shifts to 3.8 GHz approximately. This is due to the increase in electrical length of current without disturbing the overall dimension of the radiator. In this approach though it has obtained improvised result, by introducing a slot on ground plane at optimum place, we have achieved UWB in step-4.

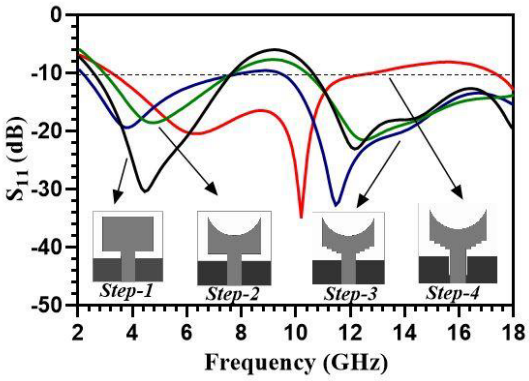

Figure 2. Different evaluation step of single UWB antenna element.

2.2. Evolution of UWB MIMO Antenna

Design-1, shown in Figure 3(a), is designed with a basic rectangular patch and a modified ground structure in which the reflection coefficient at all four ports is found to be lower than −10 dB from 2.26–11.70 GHz, but isolation parameters S_{12}, S_{13} and S_{14} are very poor in the whole UWB. To improvise the bandwidth and isolation further, we make necessary changes in design-1 by cutting a staircase shape at both the lower corners of radiators to get design-2 in Figure 3(b). For further improvement of isolation and bandwidth, design-3 shown in Figure 3(c) is designed with optimum dimensions listed in Table 2, in which cutting the rectangular slot on ground plane at optimum position leads to the change in surface current distribution whereas cutting the arc on radiator leads to improvement in the isolation without using any additional decoupling network. In all three designs, the antenna elements are placed orthogonally for isolation improvement.

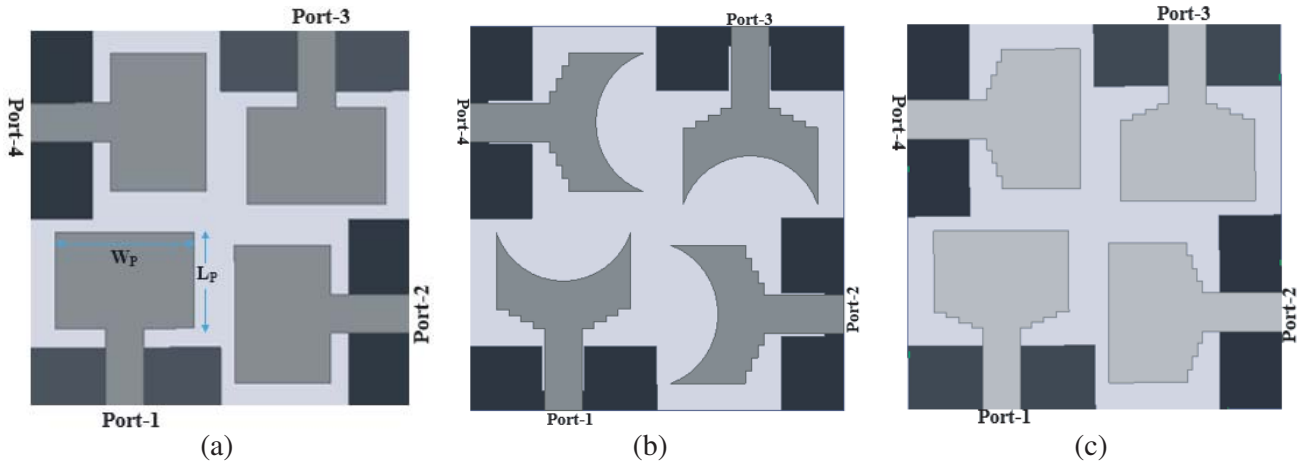

Figure 3. Geometry of rectangular patch. (a) Design-1: with modified ground. (b) Design-2: with staircase shape at corner of patch. (c) Design-3: with introducing slot on ground and arc on radiator.

The simulated S-parameters of all three designs when port-1 is excited are presented in Figure 4. Table 3 presents the range of operating frequency and value of isolation parameter of all three antennas. It is evident from the table that design-3 has the widest bandwidth (14.6 GHz) and very good isolation among all three designs.

Table 3. Comparisons of S-parameter of all three design.

Parameter	Design-1	Design-2	Design-3 (proposed antenna)
S_{11}	< -10 dB (2.26–11.70) GHz	< -10 dB (2.95–12.75) GHz	< -10 dB (2.15–16.75) GHz
S_{12}	< -14.2 dB	< -16.5 dB	< -22 dB
S_{13}	< -11 dB	< -12 dB	< -16 dB
S_{14}	< 14.11 dB	< -16.75 dB	< -23 dB

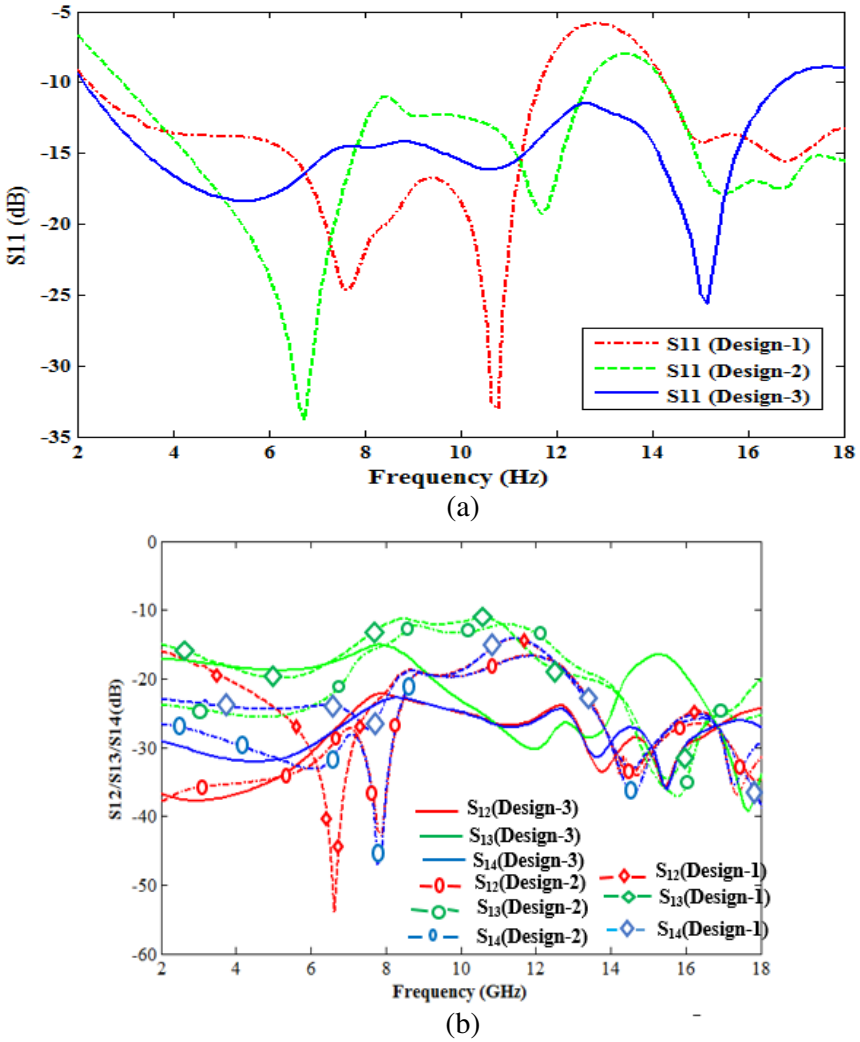

Figure 4. Comparison of S-parameter of all three design. (a) Return loss. (b) Isolation parameters.

2.3. Effect of Ground Plane

The use of partial ground plane reduces the amount of energy stored in the substrate. As a consequence, quality factor has been reduced, and it is quite obvious that bandwidth naturally will increase as quality factor is inversely proportional to bandwidth. Etching a slot on ground plane increases electrical path

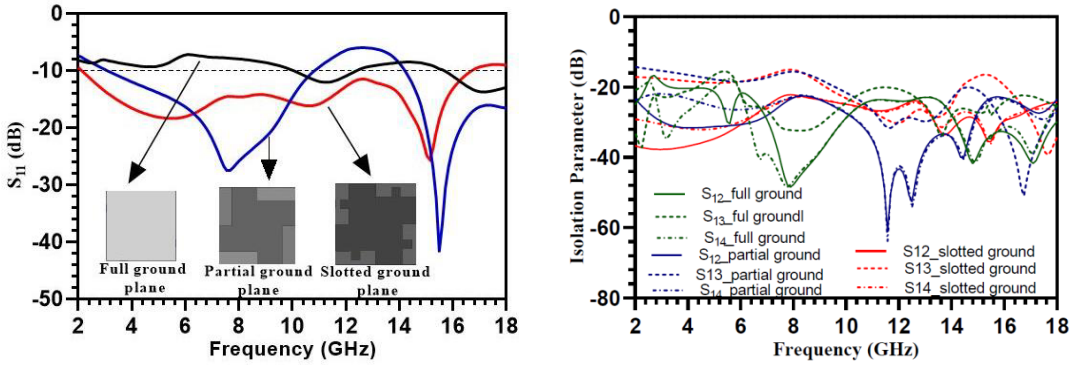

Figure 5. Effect of ground plane at various steps (a) S_{11}, (b) isolation parameter.

length of the current which increases bandwidth. In addition, the antenna also gets miniaturized. The results of return loss and isolation parameter for different steps of ground plane are illustrated in Figure 5. It can be found that the MIMO antenna with slotted ground plane provides high impedance bandwidth along with very good isolation.

3. RESULTS AND DISCUSSION

The front and back sides of prototype of four port MIMO antenna are presented in Figures 6(a) and 6(b), respectively.

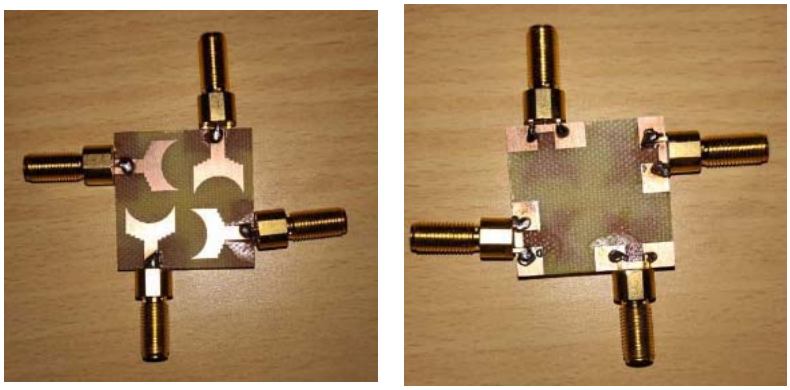

Figure 6. Fabricated prototype antenna. (a) Front side. (b) Back side.

The antenna is fabricated on an FR4 substrate with a thickness of 1.6 mm. The measurement of antenna parameters was carried on Agilent N5230A vector network analyzer. Figures 7 and 8 illustrate the comparison of measured and simulated S-parameters, and mutual coupling parameters with good agreement are set up between them. As per FCC requirement for UWB (3.1–10.6), this prototype antenna finds a larger bandwidth (2.15–16.75 GHz) than UWB. The high isolation is achieved between the first and second, and first and fourth elements which are found to be $S_{12} < -22$ dB and and $S_{14} < -23$ dB, respectively.

Figure 9 represents the two-dimensional radiation pattern of proposed MIMO antenna in E-plane and H-plane directions at 3.07, 5.37, 10.66, and 15.14 GHz. It is evident from Figure 8 that for the entire range of frequency band, the radiation pattern follows an omnidirectional characteristic.

The gain of antenna first decreases then increases up to resonance frequency 5.37 GHz and further decreases then increases up to another resonance frequency 10.66 GHz. The gain finally reaches the

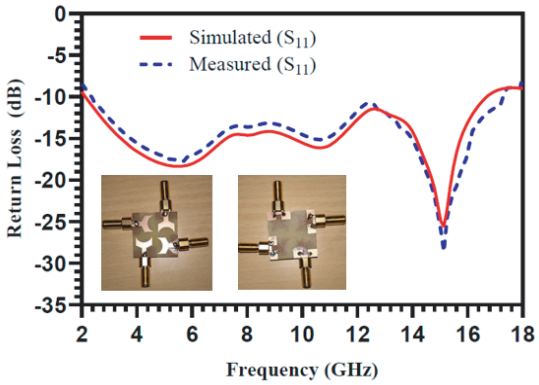

Figure 7. Simulated and measured S_{11} parameter of prototype MIMO antenna.

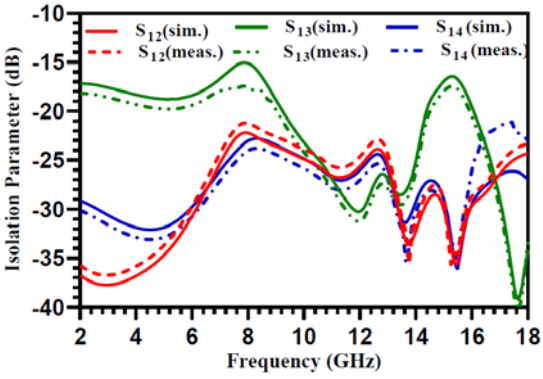

Figure 8. Comparison of isolation parameter $S_{12}/S_{13}/S_{14}$.

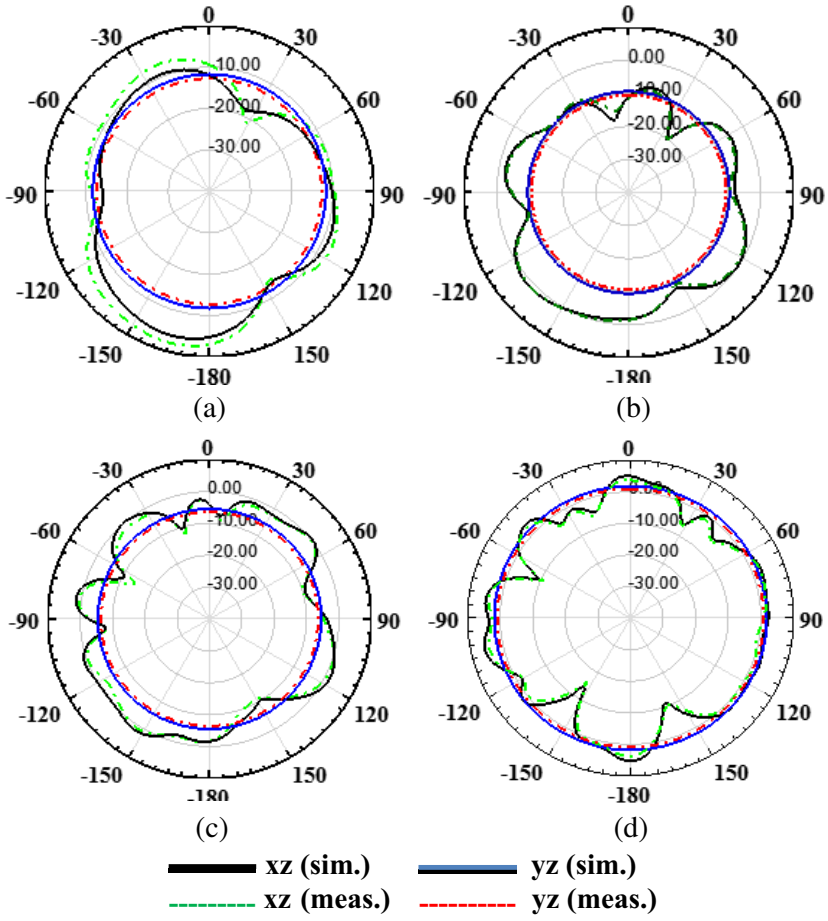

Figure 9. Radiation pattern at (a) 3.07, (b) 5.37, (c) 10.66, and (d) 15.14 GHz in xz and yz plane.

maximum value at resonance frequency 15.14 GHz. The maximum measured gain 4.8 dB and simulated gain 5 dB are achieved. It can be seen from Figure 8 that the measured gain of antenna varies from 1.2 dB to 4.8 dB. The measured and simulated radiation efficiencies of the proposed antenna have more than 60% through mthe entire frequency band as illustrated in Figure 10(b). The efficiency of antenna first increases up to 90% then further decreases and after that increases to peak value 96%. Figure 11

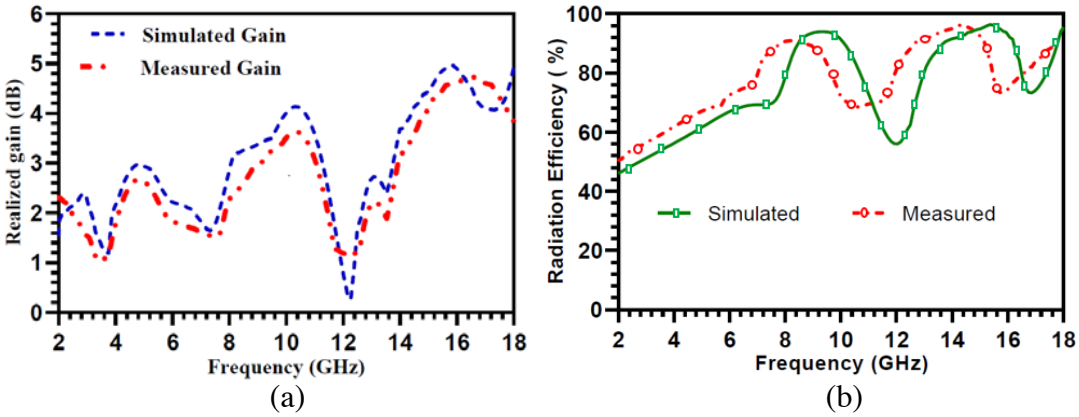

Figure 10. Comparison of (a) realized gain, (b) realized efficiency of prototype MIMO antenna.

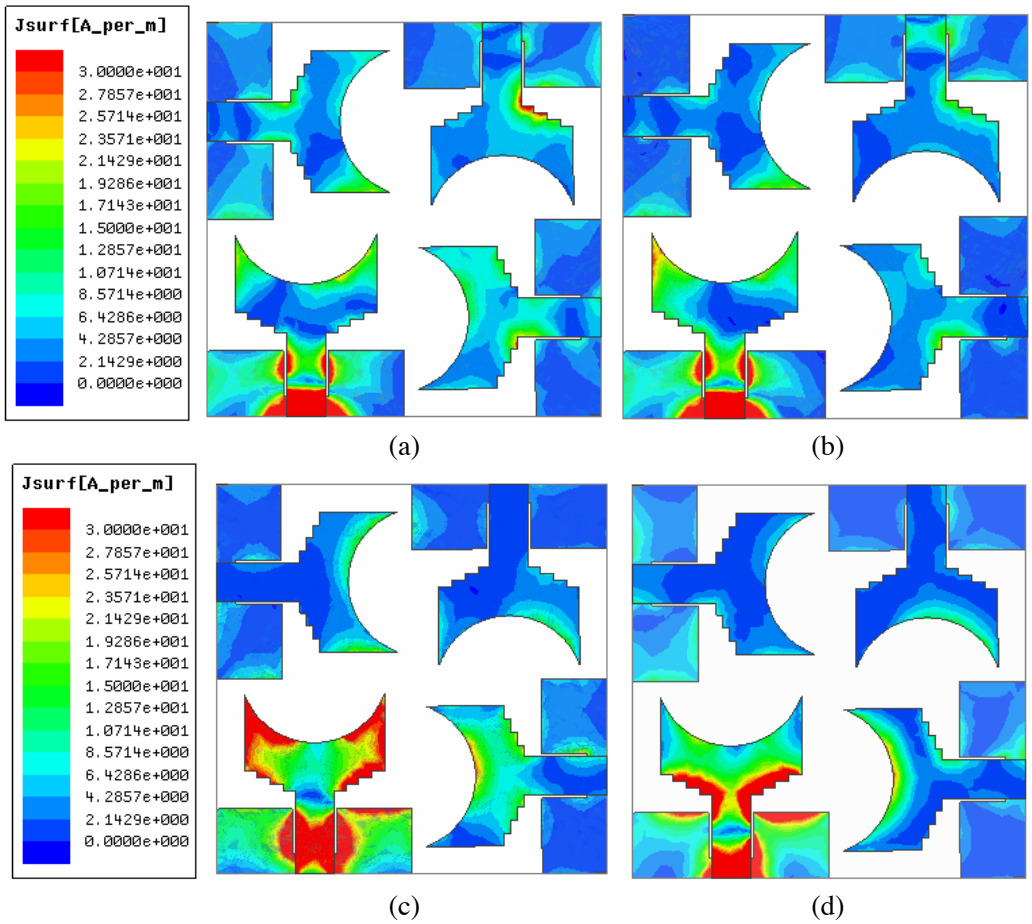

Figure 11. Surface current at (a) 3.07 GHz, (b) 5.37 GHz, (c) 10.66 GHz, (d) 15.14 GHz.

presents the surface current distribution at 3.07, 5.37, 10.66, and 15.14 GHz, respectively when port 1 is excited, and other ports are terminated with 50 ohm impedance. It can be observed that at all frequencies very small amount of current is coupled with other elements, and this is due to orthogonal arrangement of antenna elements.

4. MIMO DIVERSITY ANALYSIS

The performance of MIMO antenna cannot be fully categorized only by return loss and isolation parameters. Other parameters like ECC, diversity gain, TARC, and mean effective gain are also used to evaluate the performance of MIMO antenna.

4.1. Envelope Correlation Coefficient

It is a very important diversity parameter which categorizes the mutual coupling between antenna elements. There are two ways to evaluate ECC, using far field radiation pattern and S-parameter [26],

$$ECC = \rho_e(i,j,N) = \frac{\left|\sum_{n=1}^{N} S_{i,n}^{*} S_{n,j}\right|^2}{\left|\Pi_{k=i.j}\left(1 - \sum_{n=1}^{N} S_{k,n}^{*} S_{n,k}\right)\right|} \tag{2}$$

where i and j are the port number, and N = number of antenna elements.

Fora quad-port MIMO antenna, ECC between antenna elements can be evaluated by putting $N = 4$ in Eq. (1).

$$\mathrm{ECC}_{12} = \frac{\left|S_{11}^{*}S_{12} + S_{21}^{*}S_{22} + S_{13}^{*}S_{32} + S_{14}^{*}S_{42}\right|^2}{\left(1 - |S_{11}|^2 - |S_{21}|^2 - |S_{31}|^2 - |S_{41}|^2\right)\left(1 - |S_{12}|^2 - |S_{22}|^2 - |S_{32}|^2 - |S_{42}|^2\right)} \tag{3}$$

where ECC_{12} is the mutual coupling on port 1 due to port 2. Similarly, we can evaluate ECC_{13} and ECC_{14} from Eq. (1). It can be seen from Figure 12 that ECC value is lower than 0.065 in the whole operating band. The measured value is very low compared to practical acceptable value 0.5. It means that the MIMO antenna shows very good diversity performance.

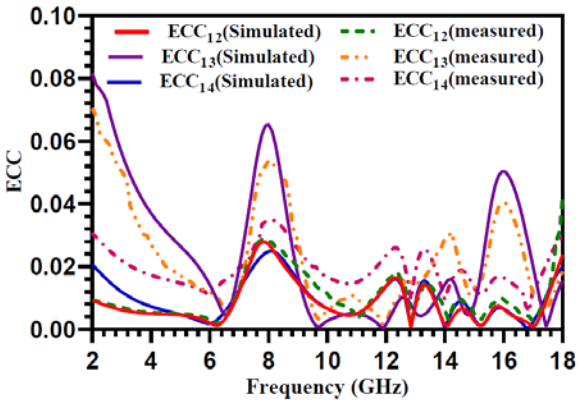

Figure 12. Envelope correlation coefficient with frequency.

4.2. Diversity Gain

The diversity gain should be close to 10 dB for effective performance of MIMO antenna as it can be directly calculated from ECC value. The DG of designed antenna is evaluated by [27],

$$\mathrm{DG} = 10\sqrt{1 - \mathrm{ECC}^2} \tag{4}$$

Figure 13 shows the diversity gain when port 1 is excited, and the other port is terminated. It is observed that the DG values in all the three cases are more than 9.98 dB which is greater than practical accepted value 9.5.

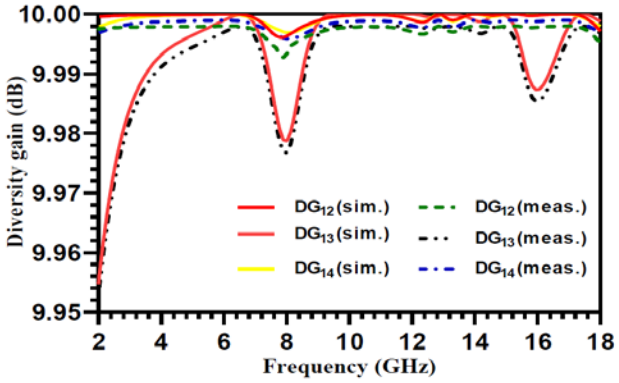

Figure 13. Diversity gain with frequency.

4.3. Total Active Reflection Coefficient

In MIMO system, operating bandwidth and efficiency will be affected when all the antenna elements operate simultaneously. Thus, S-parametric results are not sufficient to judge how good the antenna is, so we also used another important parameter known as TARC to evaluate the antenna performance. TARC can be evaluated by [6],

$$TARC = \frac{\sqrt{\sum_{i=1}^{4}) |R_i|^2)}}{\sqrt{\sum_{i=1}^{4} |I_i|^2}} \tag{5}$$

where R_i is the reflected signal, and I_i is the incident signal.

In the proposed MIMO antenna, consider that all incoming signals at all ports have the same amplitude and phase (0° phase difference), then the equation for TARC is given by [6].

$$TARC = \frac{\sqrt{|S_{11}+S_{12}+S_{13}+S_{14}|^2+|S_{21}+S_{22}+S_{23}+S_{24}|^2+|S_{31}+S_{32}+S_{33}+S_{34}|^2+|S_{41}+S_{42}+S_{43}+S_{44}|^2}}{\sqrt{4}} \tag{6}$$

It can be seen from Figure 14 that the TARC value is lower than −10 dB which is lower than practical accepted value 0 dB over the entire frequency band.

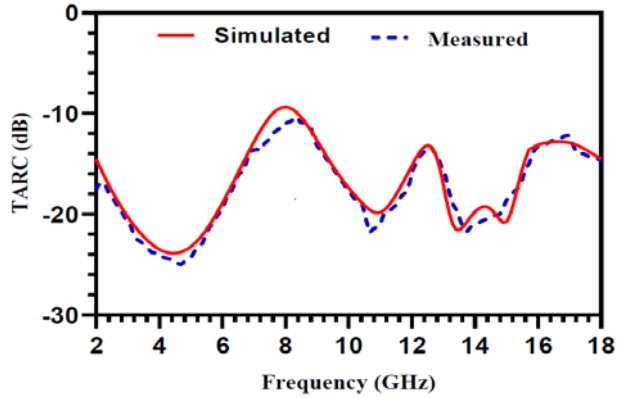

Figure 14. Simulate and measured TARC with frequency.

4.4. Mean Effective Gain

For MIMO diversity performance, MEG is also a very important parameter. It is the ratio of average power of outgoing signal to incoming signal. MEG at each port can be evaluated as [28].

$$MEG_i = 0.5\left[1 - \sum_{j=1}^{N} |S_{ij}|^2\right] \tag{7}$$

For the effective performance of MIMO antenna, the MEG should be below −3 dB at each port, and magnitude of difference of MEG between any ports should be below 3 dB. It is clear from Figure 15

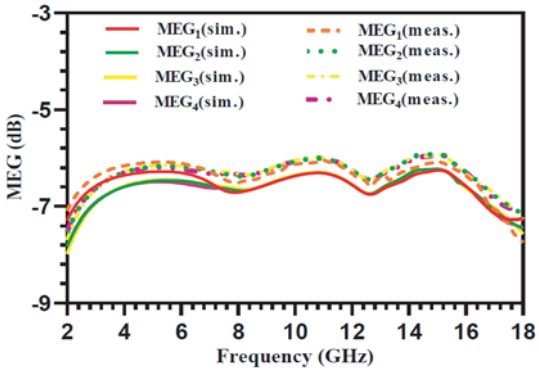

Figure 15. Simulated and measured MEG with frequency.

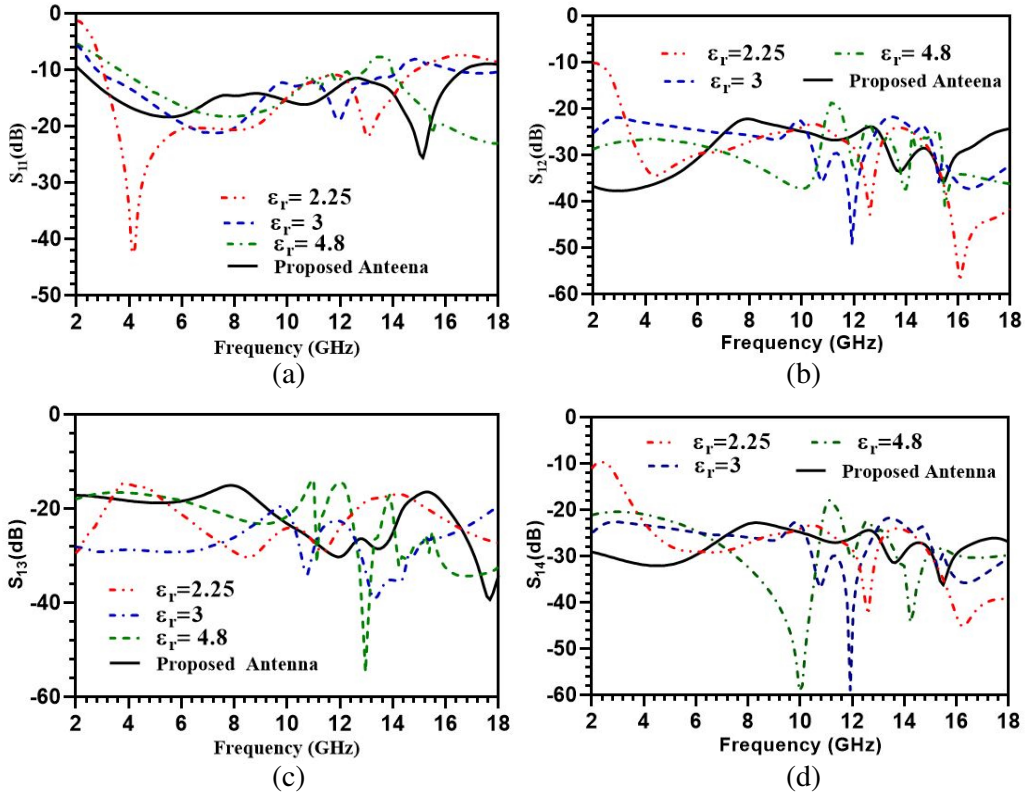

Figure 16. Comparison of S-parameter for different plastic material with proposed MIMO antenna. (a) Return loss, (b), (c) and (d) isolation parameter.

that the MEG at each port is less than −6 dB in the whole frequency band. The magnitude of difference of MEG between any ports is also within 1 dB.

4.5. Effect of Device Housing

The proposed antenna is placed inside three different plastic materials whose permittivity values are 2.25, 3 and 4.48. The size of the plastic housing is taken same as the size of the antenna, i.e., $30 \times 30\,\text{mm}^2$. The height and thickness of the box are taken as 15 mm and 1 mm, respectively. Figure 16(a) shows that the lower frequency band shifts downward as ε_r value decreases from 4.48 to 2.2, and isolation parameters S_{12}, S_{13}, and S_{14} are less than −20 dB as illustrated in Figures 16(b), (c), and (d). So the proposed antenna will satisfactorily work with different device housings.

5. CONCLUSION

A very compact $30 \times 30\,\text{mm}^2$ quad port high performance UWB MIMO antenna has been proposed. The design provides an excellent isolation ($S_{12} < -22$ dB and $S_{13} < -23$ dB) which is an essential ingredient as far as MIMO antenna is concerned. This was possible just by positioning all the antennas in an orthogonal fashion. Cutting arc on radiator and modifying the ground structure with staircase-shaped cuts at both the lower corners of patch boosted the isolation to a greater extent which is expected in MIMO environment. The proposed design is meant to have a high performance UWB MIMO antenna. This is due to various MIMO diversity parameter as well as high impedance bandwidth (2.15–16.75 GHz). The measured MIMO diversity parameters ECC, DG, and TARC were also within acceptable practical limit in the entire UWB range. Therefore, the designed antenna is a good candidate for various handheld portable devices.

REFERENCES

1. "Revision of part 15 of the commissions rules regarding ultra-wideband transmission systems first report and order," Tech. Rep. FCC 02.V48, Federal Commun. Commission, Washington, DC, USA, 2002.
2. Tao, J. and Q. Feng, "Compact ultrawideband MIMO antenna with half-slot structure," *IEEE Antennas Wirel. Propag. Lett.*, Vol. 16, 792–795, 2017.
3. Khan, M. S., A. D. Capobianco, A. M. Asif, D. E. Anagnostu, R. M. Shubair, and B. D. Braaten, "A compact CSRR-enabled UWB diversity antenna," *IEEE Antennas Wirel. Propag. Lett.*, Vol. 16, 808–812, 2017.
4. Khan, M. S., A. D. Capobianco, A. Iftikhar, R. M. Shubair, D. E. Anagnostou, and B. D. Braaten, "Ultra-compact dual-polarised UWB MIMO antenna with meandered feeding lines," *IET Microw. Antennas Propag.*, Vol. 11, No. 7, 997–1002, 2017.
5. Bilal, M., R. Saleem, H. H. Abbasi, M. F. Shafique, and A. K. Brown, "An FSS-based nonplanar quad-element UWB-MIMO antenna system," *IEEE Antennas Wirel. Propag. Lett.*, Vol. 16, 987–990, 2017.
6. Tiwari, R. N., P. Singh, B. K. Kanaujia, and K. Srivastava, "Neutralization technique based two andfour port high isolation MIMO antennas for UWB communication," *Int. J. Electron. Commun.*, Vol. 110, 152828–152837, 2019.
7. Dabas, T., D. Gangwar, B. K. Kanaujia, and A. K. Gautam, "Mutual coupling reduction between elements of UWB MIMO antenna using small size uniplanar EBG exhibiting multiple stop bands," *Int. J. Electron. Commun.*, Vol. 93, 32–38, 2018.
8. Wu, W., B. Yuan, and A. Wu, "A quad-element UWB-MIMO antenna with band-notch and reduced mutual coupling based on EBG structures," *Int. J. Antennas Propag.*, Vol. 8490740, 1–10, 2018.
9. Tang, X., Z. Yao, Y. Li, W. Zong, G. Liu, and F. Shan, "A high performance UWB MIMO antenna with defected ground structure and U-shape branches," *Int. J. RF Microw. Comput. Aided Engg.*, Vol. 22270, 1–14, 2020.

10. Wang, E., W. Wang, X. Tan, Y. Wu, J. Gao, and Y. Liu, "A UWB MIMO slot antenna using defected groundstructures for high isolation," *Int. J. RF Microw. Comput. Aided Engg.*, Vol. e22155, 1–10, 2020.
11. Deng, J. Y., L. X. Guo, and X. L. Liu, "An ultrawideband MIMO antenna with a high isolation," *IEEE Antennas Wirel. Propag. Lett.*, Vol. 15, 182–185, 2016.
12. Srivastava, G. and A. Mohan, "Compact dual-polarized UWB diversity antenna," *Microw. Opt. Technol. Lett.*, Vol. 57, No. 12, 2951–2955, 2015.
13. Ren, J., W. Hu, Y. Yin, and R. Fan, "Compact printed MIMO antenna for UWB applications," *IEEE Antennas Wirel. Propag. Lett.*, Vol. 13, 1517–1520, 2014.
14. Zhang, S., Z. Ying, J. Xiong, and S. He, "Ultrawideband MIMO/diversity antennas with a tree-like structure to enhance wideband isolation," *IEEE Antennas Wirel. Propag. Lett.*, Vol. 8, 1279–1282, 2009.
15. Lin, G. S., C. H. Sung, J. L. Chen, L. S. Chen, an M. P. Houng, "Isolation improvement in UWB MIMO antenna system using carbon black film," *IEEE Antennas Wirel. Propag. Lett.*, Vol. 16, 222–225, 2017.
16. Zhao, J. and J. Wang, "Correlation reduction in antennas with metamaterial based on newly designed SRRs," *Asia-Pacific Int. Symp. Electromagn. Compat.*, 981–984, 2010.
17. Ketzaki, D. A. and T. V. Yioultsis, "Metamaterial-based design of planar compact MIMO monopoles," *IEEE Trans. Antennas Propag.*, Vol. 61, No. 5, 2758–2766, 2013.
18. Hasan, M. N., S. Chu, and S. Bashir, "A DGS monopole antenna loaded with U-shape stub for UWB MIMO applications," *Microw. Opt. Technol. Lett.*, Vol. 61, 2141–2149, 2019.
19. Tang, X., Z. Yao, Y. Li, W. Zong, G. Liu, and F. Shan, "A high performance UWB MIMO antenna with defected ground structure and U-shape branches," *Int. J. RF Microw. Comput. Aided Engg.*, Vol. 22270, 1–14, 2020.
20. Ali, W. A. E. and A. A. Ibrahim, "A compact double-sided MIMO antenna with an improved isolation for UWB applications," *Int. J. Electron. Commun.*, Vol. 82, 7–13, 2017.
21. Zhang, J. Y., F. Zhang, and W. P. Tian, "Compact 4-port ACS-fed UWB-MIMO antenna with shared radiators," *Progress In Electromagnetics Research*, Vol. 55, 81–88, 2015.
22. Toktas, A. and A. Akdagli, "Compact multiple-input multiple-output antenna with low correlation for ultra-wideband applications," *IET Microw. Antennas Propag.*, Vol. 9, 822–829, 2015.
23. Khan, S. M., A. Iftikhar, S. M. Asif, A. D. Capobianco, and B. D. Braaten, "A compact four elements UWB MIMO antenna with on-demand WLAN rejection," *Microw. Opt. Tech. Lett.*, Vol. 58, No. 2, 270–276, 2016.
24. Tang, Z., X. Wu, J. Zhan, S. Hu, Z. Xi, and Y. Liu, "Compact UWB-MIMO antenna with high isolation and triple band-notched characteristic," *IEEE Access*, Vol. 7, 19856–19865, 2019.
25. Thomas, K. G. and M. Sreenivasan, "A simple ultrawideband planar rectangular printed Antenna with band dispensation," *IEEE Trans. Antennas Propag.*, Vol. 58, No. 1, 27–34, 2010.
26. Yussuf, A. A. and S. Paker, "Design of a compact quad-radiating element MIMO antenna for LTE/Wi-Fi application," *Int. J. Electron. Commun.*, Vol. 111, 152983–152902, 2019.
27. Chandel, R., A. K. Gautam, and K. Rambabu, "Tapered fed compact UWB MIMO-diversity antenna with dual band-notched characteristics," *IEEE Trans. Antennas Propag.*, Vol. 66, No. 4, 1677–1684, 2018.
28. Thakur, E., N. Jaglan, and S. D. Gupta, "Design of compact UWB MIMO antenna with enhanced bandwidth," *Progress In Electromagnetics Research C*, Vol. 97, 83–94, 2019.